Submitted to The Astrophysical Journal

How Hot is the Wind from TW Hydrae?[1]

Christopher M. Johns–Krull

Department of Physics & Astronomy, Rice University, 6100 Main St. MS-108, Houston, TX 77005

cmj@rice.edu

Gregory J. Herczeg

California Institute of Technology, MC105-24, 1200 East California Boulevard, Pasadena, CA 91125

gregoryh@astro.caltech.edu

ABSTRACT

It has recently been suggested that the winds from Classical T Tauri stars in general, and the wind from TW Hya in particular, reaches temperatures of at least 300,000 K while maintaing a mass loss rate of $\sim 10^{-11}$ $M_{\odot}yr^{-1}$ or larger. If confirmed, this would place strong new requirements on wind launching and heating models. We therefore re-examine spectra from the Space Telescope Imaging Spectrograph aboard the Hubble Space Telescope and spectra from the Far Ultraviolet Spectroscopic Explorer satellite in an effort to better constrain the maximum temperature in the wind of TW Hya. We find clear evidence for a wind in the C II doublet at 1037 Å and in the C II multiplet at 1335 Å. We find no wind absorption in the C IV 1550 Å doublet observed at the same time as the C II 1335 Å line or in observations of O VI observed simultaneously with the C II 1037 Å line. The presence or absence of C III wind absorption is ambiguous. The clear lack of a wind in the C IV line argues that the wind from TW Hya

[1]Based on observations with the NASA/ESA Hubble Space Telescope, obtained at the Space Telescope Science Institute, which is operated by the Association of Universities for Research in Astronomy, Inc. under NASA contract NAS5-26555. These observations are associated with program #GTO-7718. Also based on bservations made with the NASA-CNES-CSA Far Ultraviolet Spectroscopic Explorer, which is operated for NASA by the Johns Hopkins University under NASA contract NAS5-32985.

does not reach the 100,000 K characteristic formation temperature of this line. We therefore argue that the available evidence suggests that the wind from TW Hya, and probably all classical T Tauri stars, reaches a maximum temperature in the range of 10,000 – 30,000 K.

Subject headings: accretion, accretion disks — stars: individual (TW Hya) — stars: pre–main-sequence — stars: mass loss

1. Introduction

Mass loss in the form of a wide-angle wind and/or collimated jet is a common feature observed in young, low mass stars that are still surrounded by accretion disks (for a review see Bally, Reipurth, and Davis 2006). The material in these disks eventually accretes onto the central star, gets ejected in an outflow, or is incorporated into planets or other solar sytem-like bodies. Understanding the processes through which young stars interact with and eventually disperse their disks is critical for understanding the rotational evolution of stars and the formation of planets. Mass loss appears to be a necessary component in the accretion process both observationally as mentioned above and theoretically: angular momentum must be carried away in order to allow disk and stellar accretion to occur, and magnetized winds are efficient at removing angular momentum (e.g. Pudritz, Pelletier, and Gomez de Castro 1991, Shu et al. 1994).

Signatures of mass loss are observed primarily in optical, infrared, and radio wavelength spectral diagnostics. Bipolar outflows are observed in millimeter wavelength CO lines and other molecular tracers in the mm and sub-mm range (e.g. see review by Arce et al. 2006). In the infrared, emission in H_2 (e.g. Gueth & Guilloteau 1999; Stanke, McCaughrean, & Zinnecker 2002) and [Fe II] (e.g. Reipurth et al. 2000) lines are regularly seen in outflows from young stars. At optical wavelengths, Herbig-Haro (HH) objects and their associated stellar jets are routinely imaged in narrow band filters centered on Hα or on a host of forbidden lines. High resolution images of the central engine show that these jets originate from young stars surrounded by circumstellar disks, with the jet usually emerging perpendicular to the disk such as clearly seen in the case of HH 30 (Burrows et al. 1996, Ray et al. 1996). Spectroscopically, winds and jets are diagnosed by the appearance of P-Cygni like line profiles in permitted lines such as Hα (and other Balmer lines) and Na D (e.g. Mundt 1984; Reipurth. Pedrosa, & Lago 1996; Alencar & Basri 2000), and in the profiles of forbidden lines which often show a strong asymmetry with substantial blue-shifted emission with little or no red-shifted emission (e.g. Edwards et al. 1987, Hamann 1994). More recently, jets and winds from CTTSs have been detected at shorter wavelengths corresponding to higher

temperature emissions. Hartigan et al. (1999) detect several ultraviolet (UV) Fe II emission lines in the HH 47A bow shock, and several irradiated jets with UV signatures have been discovered recently (e.g. Reipurth et al. 1998, Bally & Reipurth 2001). Gomez de Castro and Verdugo (2001) identify feature in the UV semiforbidden emission lines of C III] λ1908 and Si III] λ1892 which they associate with shocks at the base of the jet in a few CTTSs. At X-ray energies, a number of jets have also been recently detected (e.g. Pravdo et al. 2001; Favata et al. 2002; Bally, Feigelson, & Reipurth 2003). This X-ray emission forms in the fastest shocks associated with these stellar jets (see also Bally et al. 2006). While these high excitation emissions appear associated with shocks within the jets from young stars, until recently it was generally thought that the stellar or disk wind at the base of these jets was only heated to a level which could produce features such as the the P-Cygni like profiles visible in the Balmer lines.

A hot wind component, possibly with an origin on the star as opposed to in the disk, has recently been proposed by a few authors. Beristain, Edwards, and Kwan (2001) argue for a hot wind component in CTTSs based on the analysis of high resolution He I and He II line profiles observed in the optical. Takami et al. (2002) and Edwards et al. (2003) find obvious blue-shifted absorption below the local continuum in the He I λ10830 line in 6 young, low mass stars, again providing evidence for a hot wind component forming relatively near the star. Edwards et al. (2003) point out that the strength and ubiquity of this absorption indicates that the wind emanates over a large solid angle from the star: the He I λ10830 line does not trace a highly collimated flow. These results are reinforced by Edwards et al. (2006), who found subcontinuum He I λ10830 wind absorption in 26 of 38 CTTSs. The λ5876 and λ10830 lines of He I require a strong ionizing flux or a high temperature for excitation, as their upper states lie ~ 20 eV above the ground level. If these lines are primarily collisionally excited, temperatures of $\sim 25,000$ K are required to excite them (Athay 1965; Avrett, Vernazza, & Linsky 1976). With photoionization followed by recombination and cascade, helium excitation can take place at local kinetic temperatures between 8000 and 15,000 K (Zirin 1975; Heasley, Mihalas, & Poland 1974; Wahlstrom & Carlsson 1994). CTTSs in general (e.g. Feigelson et al. 2002), and TW Hya in particular (Kastner et al. 2002), are strong X-ray sources, so the detection of these He I lines in CTTS winds still leaves a wide range of possible temperatures present in these outflows. Dupree et al. (2005) detect He I λ10830 absorption in the wind from TW Hya and T Tau. They combine these observations with an analysis of the line profiles of C III λ977 and O VI λ1032 observed with the Far Ultraviolet Spectroscopic Explorer (*FUSE*) satellite to suggest that CTTSs possess continuous, smoothly accelerating winds which reach velocities of ~ 400 km s^{-1} and temperatures of $\sim 300,000$ K. These results are based primarily on the *FUSE* data for TW Hya, since the data for T Tau is much lower in quality. Dupree et al. (2005) find a

minimum mass loss rate for the O VI line of 2.3×10^{-11} $M_{\odot}yr^{-1}$.

Such a hot temperature for the wind from TW Hya is surprising, particularly given the high mass loss rate. Alencar & Batalha (2002) and Herczeg et al. (2004) estimate a mass accretion rate onto TW Hya of $\sim 2 \times 10^{-9}$ $M_{\odot}$ yr^{-1}. Most estimates suggest that the mass loss rate from CTTSs is 0.1 – 0.3 times that of the mass accretion rate (Königl & Pudritz 2000, Shu et al. 1994), suggesting the mass loss rate from TW Hya may be as high as 5×10^{-10} $M_{\odot}$ yr^{-1}. Such a high temperature, high mass loss rate wind puts strong constraints on the ultimate origin and heating of winds from CTTSs. Current theories of mass loss from CTTSs primarily produce cold, magnetocentrifugally driven flows from the disks around these stars (e.g. Königl & Pudritz 2000, Shu et al. 2000) which are then heated by a combination of ambipolar diffusion and X-rays to temperatures of $\sim 10^4$ K (Shang et al. 2002; Shang, Li, & Hirano 2006). Photoevaporation of the surface layer of the disk may also produce a low velocity (~ 10 km s^{-1}) wind with a characteristic temperature of 10^4 K as well (e.g. Matsuyama, Johnstone, & Hartmann 2003; Font et al. 2004). Thus, if the Dupree et al. (2005) suggestion holds true, a totally new heating, and possibly driving, mechanism must be identified. The analysis presented by Dupree et al. (2005) relies on the asymmetric *shape* of the line profiles tracing the hot gas: no true absorption against a local continuum is detected. Therefore, we re-examine the published (Herczeg et al. 2002, 2004; Dupree et al. 2005) high resolution spectra from the Space Telescope Imaging Spectrograph (*STIS*) aboard the Hubble Space Telescope (*HST*) and from the *FUSE* satellite to look for firm wind signatures and confirm the high proposed temperature in the wind of TW Hya. The *STIS* and *FUSE* bandpasses cover several lines with characteristic formation temperatures ranging from $\sim 10^4$ K to $\sim 300,000$ K. We find firm evidence against the proposed wind in the C IV and O VI lines of TW Hya. We therefore conclude that the wind in fact does not reach (at least at large optical depth as claimed) a temperature of $\sim 100,000$ K, characteristic of the formation of the C IV line. In §2 we describe the observational data. Section 3 presents our analysis, and §4 gives a discussion of our results.

2. Observations and Data Reduction

We observed TW Hya with the E140M echelle grating and the $0\farcs5 \times 0\farcs5$ aperture on *HST*/STIS for 2.3 ks as part of *HST* program GTO-7718. The spectrum spans from 1170–1700 Å with $R = 25,000$. The data were reduced using standard calSTIS reduction package written for *IDL*. The flux calibration is accurate to $\sim 10\%$. The wavelength calibration is accurate to ~ 5 km s^{-1}. This spectrum was described by Herczeg et al. (2002).

We also observed TW Hya with the LWRS ($30''$) aperture on *FUSE* for a total of 32.8 ks

in programs GO-C067 and GTO-P186. The *FUSE* consists of four co-aligned telescopes, each of which have two channels coated with LiF and SiC (Moos et al. 2000). Each observation yields eight independent spectra covering ~ 90 Å. Our co-added spectrum spans from 905–1187 Å with $R \sim 15,000$.

We reduced the *FUSE* spectra using version 3.1.3 of the calFUSE standard data reduction pipeline[1]. Pulse height values for each LiF and SiC spectrum were restricted to those detected in the individual extraction windows to reduce background noise. We use the standard calFUSE wavelength solution; however, the zero-point for this solution is not correct and must be fixed using the observed spectrum. We calibrated wavelengths at $\lambda > 1000$ Å using 25 different H_2 lines in this region, setting the wavelength zero point so that these lines appear at the radial velocity of the star (Herczeg et al. 2002). We calibrated the zero point of wavelengths at $\lambda < 1000$ Å by cross-correlating the emission profiles for the N III 991.5 Å lines and several O I airglow lines, which appear in both the longer (calibrated with the H_2 lines) and shorter-wavelength channels that overlap between 985–1005 Å. The error in our wavelength solution is ~ 10 km s^{-1} at $\lambda > 1000$ Å and ~ 15 km s^{-1} at $\lambda < 1000$ Å. The absolute and relative flux calibration is accurate to $\sim 10\%$ and $\sim 5\%$, respectively, at wavelengths discussed in this paper. The background subtraction is accurate to $0.5-3\times10^{-15}$ erg cm^{-2} s^{-1} Å^{-1}. To reduce possible contamination by airglow lines, we restrict our analysis to data obtained during *FUSE* nighttime.

3. Analysis

3.1. Wind Absorption of H_2 and Below the Local Continuum

Dupree et al. (2005) assert the presence of a hot ($\sim 300,000$ K) wind from TW Hya based on the *shape* of O VI and C III emission line profiles. When considering the shape of emission lines, there can be an ambiguity between self-absorption in some part of the line profile and simply a lack of emission in this same part of the profile. The presence of a wind is much more firmly deduced when absorption is detected against a local continuum. Contrary to the statements in Dupree et al. (2005), a UV continuum is detected from TW Hya, as is evident in many of the figures shown Herczeg et al. (2002) based on *STIS* data. This continuum is clearly visible in Figures 1 and 3. Also evident in Figure 1 is that the flux goes to zero in blueshifted wind absorption profiles for key lines from both the *STIS* and *FUSE* spectra.

[1]http://fuse.pha.jhu.edu/analysis/calfuse.html

All of the strong, unblended, relatively low temperature lines present in the *STIS* spectrum of TW Hya, including the C II 1335 Å lines, the O I 1305 Å triplet, and the Si II doublets at 1260 and 1530 Å show evidence for wind absorption below the local continuum. In the upper panel of Figure 1, we show that the wind absorption from the stronger, red members of the C II λ1335 lines[1] stays at zero flux out to a velocity of ~ -185 km s^{-1} and the flux in the wind of the weaker blue member stays at zero flux out to a velocity of -165 km s^{-1}. The lower two panels show line profiles from the *FUSE* spectrum of TW Hya which show clear absorption below the local continuum. The middle panel shows the C II λ1037 doublet which is blended with the O VI λ1038 line. Absorption below the local continuum is detected in this C II doublet and in H I Lyβ, which are both adjacent to the O VI lines. The blue member of both the C II λ1037 doublet and the C II λ1335 multiplet suffers wind absorption by the red members (see also §3.2). To quantify the above, we present in Table 1 continuum measurements near each of the lines of interest discussed here. The continuum in each region is detected at a very significant level, whereas in the wind absorption region of C II λ1335.7 for example, the measured flux is $1.2 \pm 0.7 \times 10^{-15}$ ergs cm^{-2} s^{-1} Å^{-1} in the velocity range -90 to -170 km s^{-1}.

The top panel of Figure 1 also shows that the H_2 λ1333.797 line is located at -165 km s^{-1} from the C II λ1334.5 line, within the wind absorption (again, the red member of the multiplet shows the wind absorption in these lines is strong out to at least -185 km s^{-1}). Of 140 H_2 line fluxes from TW Hya modeled by Herczeg et al. (2004), this H_2 line is conspicuous in that it is the only line that is not well fit. The observed flux of 7.9 ± 0.7 erg cm^{-2} s^{-1} in this line is a factor of 6 below its predicted level. Herczeg et al. (2002) determine that the UV H_2 emission lines originate in the disk within 2 AU of the star, and Figure 1 shows that the H_2 emission is subject to wind absorption.

3.2. The Proposed Hot Wind

Dupree et al. (2005) diagnose the presence of a hot wind from TW Hya by examining the shape of the C III λ977 and O VI λ1032 emission lines. These lines display an asymmetry in their profiles such that there is more emission on the red side of the profile than on the blue. This could represent self-absorption or scattering in a wind, or an accretion flow that preferentially produces red-shifted emission. We show these and the C IV λ1548 line profiles

[1]We note that the C II λ1335 feature is a triplet with lines at 1334.532 Å, 1335.663 Å, and 1335.708 Å; however, the middle member of this triplet should be quite weak due to its low oscillator strength which is approximately an order of magnitude lower than that of the 1335.708 Å line (Kurucz & Bell 1995). Therefore, in Figure 1 we mark only the positions of the bluemost and redmost members of the multiplet.

in Figure 2. Also shown is a Gaussian fit to the right side of the line profile, as was done by Dupree et al. (2005). The Gaussian is centered at 0 km s^{-1} and its width and amplitude are fit to the red wing of the emission line profile. The red side of the C III and O VI are fairly Gaussian in shape. The C IV line is not well fit by a Gaussian, but the fitting illustrates the essential points discussed by Dupree et al. (2005). They cite the flux deficit on the blue side of the profile relative to the Gaussian fit as evidence for the hot wind. Dupree et al. (2005) then estimate the maximum velocity in the wind traced by the different diagnostics by estimating where the fit rejoins the observations in the far blue wing. For our data reductions and fits, we find velocities of ~ -275 km s^{-1}, ~ -400 km s^{-1}, and ~ -400 km s^{-1} for C III, O VI, and C IV, respectively, which are similar to the values of -325 km $s^{-1}$and -440 km s^{-1} for C III and O VI found by Dupree et al. (2005).

3.3. A Closer Look at the *STIS* C IV and C II Lines

The C IV λ1550 doublet provides three very significant clues which clearly show that there is no wind absorption in these lines. First, the profile on the blue side of the C IV does not go below the local continuum (i.e. to a flux of 0) as is the case for the wind absorption lines shown in Figure 1. One may counter that the optical depth in the C IV lines is simply lower than in the lines shown in Figure 1. The additional points address this concern.

An H_2 line at 1547.4 Å is located at a velocity of -165 km s^{-1} relative to C IV λ1548, which is well within any possible wind absorption due to C IV. This H_2 line has a measured flux of $35.3 \pm 2.7 \times 10^{-15}$ ergs cm^{-2} s^{-1} and a predicted flux of 33.0×10^{-15} ergs cm^{-2} s^{-1} (Herczeg et al. 2004). The blue wing of the C IV 1548.19 Å line in the immediate vicinity of the λ1547 H_2 line is reduced by a factor of ~ 5.5 relative to the Gaussian fit at this velocity. Dupree et al. (2005) interpret this as wind absorption in the C IV line. The discussion in §3.1 above demonstrates that the H_2 lines form inside the wind and will suffer absorption if a wind absorber overlaps a given H_2 line in wavelength. As a result, we would expect the λ1547 H_2 line to have an observed flux about a factor of ~ 5.5 below that predicted by Herczeg et al. (2004), as is in fact seen for the λ1334 H_2 line shortward of C II λ1334.5 (see §3.1). Since absolutely no absorption is detected in the λ1547 H_2 line, we conclude there is no significant wind absorption in C IV.

The third strike against a hot wind visible in the C IV lines is illustrated in Figure 3. Shown in black is the line profile for the blue components of the C II λ1335 (top panel) and the C IV (middle panel) lines. Shown in red is the red component of the respective lines overlayed and scaled to match near the peaks and in the blue wings. The two components of the C IV line have almost identical shape, which is somewhat expected since they trace

almost exactly the same material. The red wing of the 1548.19 Å line extends to ~ -130 km s^{-1} relative to the 1550.77 Å line, where any wind absorption due to the 1550.77 Å line should be quite strong. Looking at the middle panel of Figure 3, the observed flux in the 1548.19 Å line is down by a factor or ~ 5.5 at this velocity. The red wing of the 1548.19 Å line shows no such evidence for absorption due to the "wind" traced by the 1550.77 Å line.

This is not at all the case for C II, where we know there truly is a wind present. By overplotting the C II lines in the top panel of Figure 3, we see that the short wavelength (1334.53 Å) member of the multiplet shows dramatic absorption due to the wind from the long wavelength members of the multiplet. The different members of the multiplet trace essentially the same material. The red profile in the upper panel of Figure 3 show that the emission in these lines should extend to $\sim +300$ km s^{-1}; however, the 1334.53 Å line only extends to $\sim +80$ km s^{-1} due to the strong wind absorption due to the red members of the multiplet.

If these C IV lines (absorption and emission components) form in a wind, the far red wings are formed by material on the far side of the star. TW Hya has a large inner hole in its disk (e.g. Johns–Krull & Valenti 2001), so this material would be visible. If the emission component to the line forms in the magnetospheric accretion flow, it forms very near the star. Regardless of whether the emission is produced by the accretion flow or the wind, the light would pass through the wind on the near side of TW Hya and should suffer absorption at any wavelength where the projected velocities from the two lines overlap. The total lack of detectable C IV absorption again leads us to conclude there is no significant amount of C IV in the wind from TW Hya.

3.4. A Closer Look at the *FUSE* O VI and C III Lines

The O VI emission line profiles are similar to the C IV profiles, with strong redshifted emission extending to $\sim +400$ km s^{-1} and much weaker blueshifted emission. The middle panel of Figure 1 demonstrates that the continuum flux goes to zero in wind absorption due to the nearby C II λ1037 doublet and the Lyβ λ1025.7 line. However, Figures 2 and 3 demonstrate that we do not detect any subcontinuum absorption produced by the stronger member of the O VI doublet, at 1031.91 Å.

The long wavelength member of the C II λ1037 doublet occurs at -172 km s^{-1} relative to the O VI λ1037.6 line. The lower panel of Fig. 3 overlays two O VI lines, and the scaled C II λ1335.7 is used as an approximation for the C II λ1037.0 line profile. Any wind in the O VI λ1037.6 line would absorb most of the C II λ1037.0 line, but the red side of the

C II line is strong, showing no indication of absorption. We therefore find an absence of any detectable O VI in the wind.

Whether the C III line shows wind absorption is ambiguous. The sensitivity of *FUSE* at 977 Å is lower than at 1035 Å, so the continuum is not as well detected. The continuum level measured between -100 and -200 km s^{-1} from line center is $\sim 10^{-14}$ erg cm^{-2} s^{-1} $Å^{-1}$, which is higher than the local continuum of 4.5×10^{-15} erg cm^{-2} s^{-1} $Å^{-1}$. No definite C III wind absorption is detected, but we also cannot rule out some wind absorption that is either optically thin or narrower than that seen in other wind absorption lines. The non-detection is therefore ambiguous.

Some emission is present at -270 km s^{-1}, with a flux 10% that at the peak of the line profile. The flux in C IV and O VI lines drops to 10% the peak value at -150 km s^{-1}, while C II lines show no emission shortward of -200 km s^{-1}. Therefore, the emission at -270 km s^{-1} is probably not C III emission. An H_2 line at 976.2 Å may contribute as much as half of the flux at -280 km s^{-1}. We are unable to identify the additional emission as either airglow or other atomic lines. However, we are unable to use the presence of emission at -270 km s^{-1} to infer the presence of C III wind absorption.

4. Discussion

The hot FUV emission lines from CTTSs are related to accretion, as is seen in correlations with mass accretion rate (Johns–Krull et al. 2000; Calvet et al. 2004). The line profiles are often complex, and can show significant excess redshifted emission. Such an asymmetric line profile is naturally expected for optically thin lines that are produced by hot gas in downflowing accretion columns. Dupree et al. (2005) also suggest that narrow O VI profiles in the lower-quality spectrum of T Tau could suggest wind absorption, but the narrow width is instead caused by strong absorption in interstellar H_2 lines (e.g., Roberge et al. 2001, Walter et al. 2003). However, asymmetric or narrow profiles of warm emission lines, including C II-C IV, O VI, He II, N V, and Si IV are insufficient to infer the presence of a wind from CTTSs. Detecting wind absorption from FUV spectra of CTTSs requires either measuring subcontinuum absorption or absorption of nearby atomic or H_2 lines.

We conclusively find that no C IV wind absorption is detected in the STIS spectrum of TW Hya, based on several independent diagnostics. Since C IV and O VI trace gas at $T = 100,000$ and $300,000$ K, respectively, the lack of any detectable C IV in the wind means that no higher temperature O VI gas will be detectable. We confirm this conclusion by finding an absence of O VI wind absorption in the *FUSE* spectrum of TW Hya. These

findings emphasize the result that asymmetric line profiles with more red emission than blue as shown here do not necessarily diagnose the presence of a wind. Indeed, Lamzin et al. (2004) argue that the extended blue wings of C III λ977 Å, C IV λ1550 Å, and O VI λ1032 Å arise in the magnetospheric infall around TW Hya.

The lack of detectable absorption by C IV and the positive detection of C II wind absorption indicates that the abundance of C IV in the wind is less than 1% of that of C II. Based on the ionization equilibrium of C, this upper limit suggests a maximum wind temperature of $< 50,000$ K. The detection of optically thin wind absorption in the He I λ10830 Å requires either some photoionization or temperatures of $> 25,000$ K in the wind. In either case, some C III wind absorption is expected. Unfortunately the *FUSE* spectrum of TW Hya at 977 Å is not high enough quality to clearly detect the presence or absence of C III in the wind.

In addition to C II and H I discussed earlier, wind absorption from TW Hya is detected in Al II, Si II, Mg II, O I, and N I, but is not detected in C I or Si I. Wind absorption is also prevalent from the CTTS RU Lupi (Herczeg et al. 2005), which has a much higher mass accretion rate than TW Hya, and therefore presumably a higher wind mass loss rate. In addition to the same wind absorption lines as seen in TW Hya, the higher optical depth in the wind from RU Lupi allows us to detect Cl I, many Fe II lines, and Si III. The similarity in wind absorption lines from RU Lupi and TW Hya suggests that the ionization of the wind can be similar for stars with mass loss rates that likely differ by at least a factor of 10.

The absence of C I absorption in the wind of both TW Hya and RU Lupi star suggests that the temperature of the wind is $> 20,000$ K. However, the presence of O I, Cl I, and Fe II in the wind requires gas at $T < 20,000$ K. We therefore speculate that the winds from CTTSs have a kinetic temperature of $\sim 10,000$ K, and that the ionization state is dominated by photoionization. Elements with first ionization potential longward of the Lyman limit are photoionized. A smaller amount of ionising photons may also irradiate the wind, which would explain prevalent wind absorption in the He I recombination line at 10830 Å (Edwards et al. 2006), N I lines with lower levels excited to 2.4 eV, and the detection of Si III in the wind of RU Lupi (Herczeg et al. 2005). No strong lines occur between 912–954 Å, which may explain why Cl I is not ionized in the wind of RU Lupi.

We would like to acknowledge several useful comments from an anonymous referee. CMJ-K acknowledges partial support through program #AR-9933 provided by NASA through a grant from the Space Telescope Science Institute, which is operated by the Association of Universities for Research in Astronomy, Inc., under NASA contract NAS5-26555. GJH acknowledges partial support from *FUSE* program GO-C067, provided by NASA contract

NAS5-32985.

REFERENCES

Alencar, S. H. P., & Basri, G. 2000, AJ, 119, 1881

Alencar, S. H. P., & Batalha, C. 2002, ApJ, 571, 378

Arce, H. G., Shepherd, D., Gueth, F., Lee, C.-F., Bachiller, R., Rosen, A., & Beuther, H. 2006, Protostars and Planets V, B. Reipurth, D. Jewitt, & K Keil (eds.), (Tucson: Univ. of Arizona Press), in press

Athay, R. G. 1965, ApJ, 142, 755

Avrett, E. H., Vernazza, J. E., & Linsky, J. L. 1976, ApJ, 207, L199

Bally, J., Feigelson, E., & Reipurth, B. 2003, ApJ, 584, 843

Bally, J., & Reipurth, B. 2001, ApJ, 546, 299

Bally, J., Reipurth, B., & Davis, C. J. 2006, Protostars and Planets V, B. Reipurth, D. Jewitt, & K Keil (eds.), (Tucson: Univ. of Arizona Press), in press

Beristain, G., Edwards, S., & Kwan, J. 2001, ApJ, 551, 1037

Burrows, C. J., et al. 1996, ApJ, 473, 437

Calvet, N., Muzerolle, J., Briceno, C., Hernandez, J., Hartmann, L., Saucedo, J. L., & Gordon, K. D. 2004, AJ, 128, 1294

Dupree, A. K., Brickhouse, N. S., Smith, G. H., & Strader, J. 2005, ApJ, 625, L131

Edwards, D., Cabrit, S., Strom, S. E., Heyer, I., Strom, K. S., & Anerdson, E. 1987, ApJ, 321, 473

Edwards, S., Fischer, W., Hillenbrand, L., & Kwan, J. 2006, ApJ, 646, 319

Edwards, S., Fischer, W., Kwan, J., Hillenbrand, L., & Dupree, A. K. 2003, ApJ, 599, L41

Favata, F., Fridlund, C. V. M., Micela, G., Sciortino, S., & Kaas, A. A. 2002, A&A, 386, 204

Feigelson, E. D., Broos, P., Gaffney, J. A., III, Garmire, G., Hillenbrand, L. A., Pravdo, S. H., Townsley, L., & Tsuboi, Y. 2002, ApJ, 574, 258

Font, A. S., McCarthy, I. G., Johnstone, D., & Ballantyne, D. R. 2004, ApJ, 607, 890

Gómez de Castro, A. I., & Verdugo, E. 2001, ApJ, 548, 976

Gueth, F., & Guilloteau, S. 1999, A&A, 343, 571

Hamann, F. 1994, ApJS, 93, 485

Hartigan, P., Morse, J. A., Tumlinson, J., Raymond, J., & Heathcote, S. 1999, ApJ, 512, 901

Heasley, J. N., Mihalas, D., & Poland, A. I. 1974, ApJ, 192, 181

Herczeg, G. J., Linsky, J. L., Valenti, J. A., Johns–Krull, C. M., & Wood, B. E. 2002, ApJ, 572, 310

Herczeg, G. J., Wood, B. E., Linsky, J. L., Valenti, J. A., & Johns–Krull, C. M. 2004, ApJ, 607, 369

Herczeg, G. J., et al. 2005, AJ, 129, 2777

Johns–Krull, C. M. and Valenti, J. A. 2001, ApJ, 561, 1060

Johns-Krull, C. M., Valenti, J. A., & Linsky, J. L. 2000, ApJ, 539, 815

Kastner, J. H., Huenemoerder, D. P., Schulz, N. S., Canizares, C. R., & Weintraub, D. A. 2002, ApJ, 567, 434

Königl, A., & Pudritz, R. E. 2000, Protostars and Planets IV, 759

Kurucz, R. L. & Bell, B. 1995, Kurucz CD-ROM No. 23: Atomic Line Data, Cambridge, Mass.: Smithsonian Astrophysical Observatory

Lamzin, S. A., Kravtsova, A. S., Romanova, M. M., & Batalha, C. 2004, Astronomy Letters, 30, 413

Matsuyama, I., Johnstone, D., & Hartmann, L. 2003, ApJ, 582, 893

Moos, H. W., et al. 2000, ApJ, 538, L1

Mundt, R. 1984, ApJ, 280, 749

Pravdo, S. H., Feigelson, E. D., Garmire, G., Maeda, Y., Tsuboi, Y., & Bally, J. 2001, Nature, 413, 708

Pudritz, R. E., Pelletier, G., & Gomez de Castro, A. I. 1991, NATO ASIC Proc. 342: The Physics of Star Formation and Early Stellar Evolution, 539

Ray, T. P., Mundt, R., Dyson, J. E., Falle, S. A. E. G., & Raga, A. C. 1996, ApJ, 468, L103

Reipurth, B., Bally, J., Fesen, R. A., & Devine, D. 1998, Nature, 396, 343

Reipurth, B., Pedrosa, A., & Lago, M. T. V. T. 1996, A&AS, 120, 229

Reipurth, B., Yu, K. C., Heathcote, S., Bally, J., & Rodríguez, L. F. 2000, AJ, 120, 1449

Roberge, A., et al. 2001, ApJ, 551, L97

Shang, H., Glassgold, A. E., Shu, F. H., & Lizano, S. 2002, ApJ, 564, 853

Shang, H., Li, Z.-Y., & Hirano, N. 2006, Protostars and Planets V, B. Reipurth, D. Jewitt, & K Keil (eds.), (Tucson: Univ. of Arizona Press), in press

Shu, F. H., Najita, J., Ostriker, E., Wilkin, F., Ruden, S., & Lizano, S. 1994, ApJ, 429, 781

Shu, F. H., Najita, J. R., Shang, H., & Li, Z.-Y. 2000, Protostars and Planets IV, 789

Stanke, T., McCaughrean, M. J., & Zinnecker, H. 2002, A&A, 392, 239

Takami, M., Chrysostomou, A., Bailey, J., Gledhill, T. M., Tamura, M., & Terada, H. 2002, ApJ, 568, L53

Wahlstrom, C., & Carlsson, M. 1994, ApJ, 433, 417

Walter, F. M., et al. 2003, AJ, 126, 3076

Zirin, H. 1975, ApJ, 199, L163

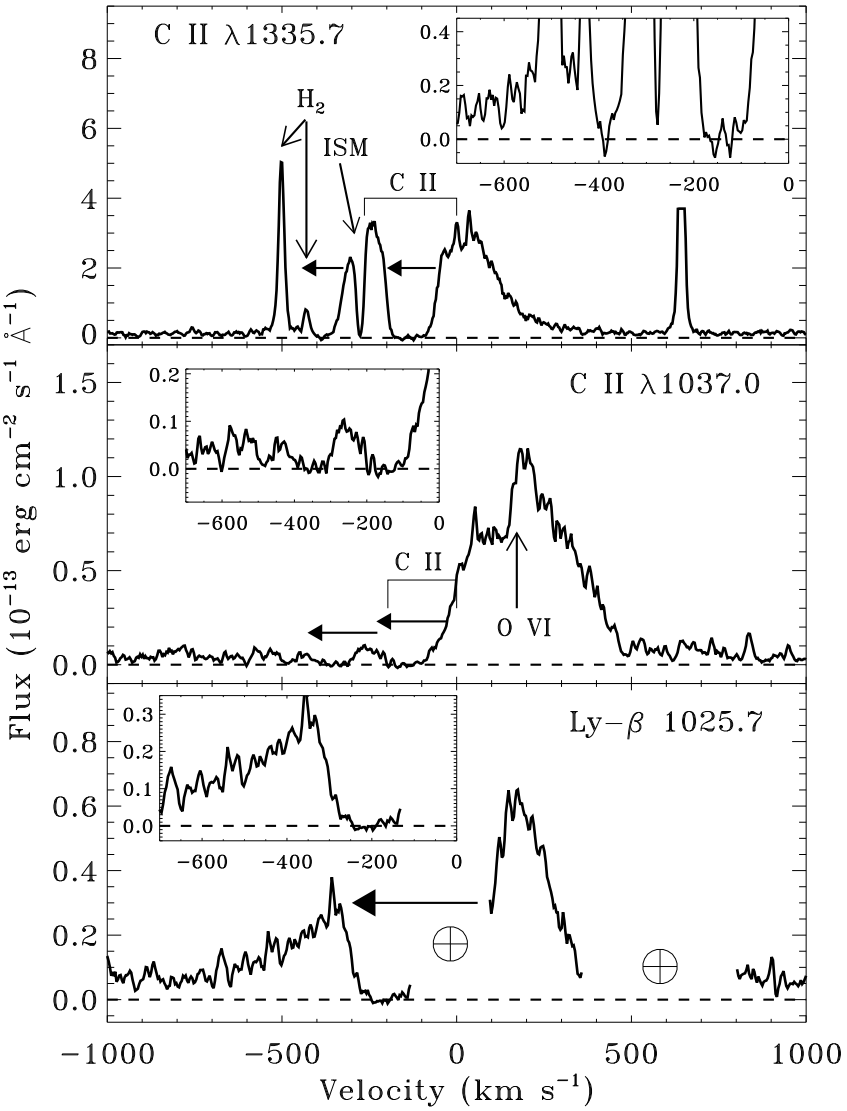

Fig. 1.— Line profiles of UV emission lines in TW Hya which show blue-shifted wind absorption below the local continuum. The C II λ1335 lines in the upper panel come from the *STIS* spectrum. The lower two panels show C II λ1037, O VI λ1038, and Ly-β lines in TW Hya observed by *FUSE*. The dashed horizontal line marks the zero flux level. Horizontal arrows indicate the range over which wind absorption is detected. The inserts clearly show this wind absorption below the local continuum in each line.

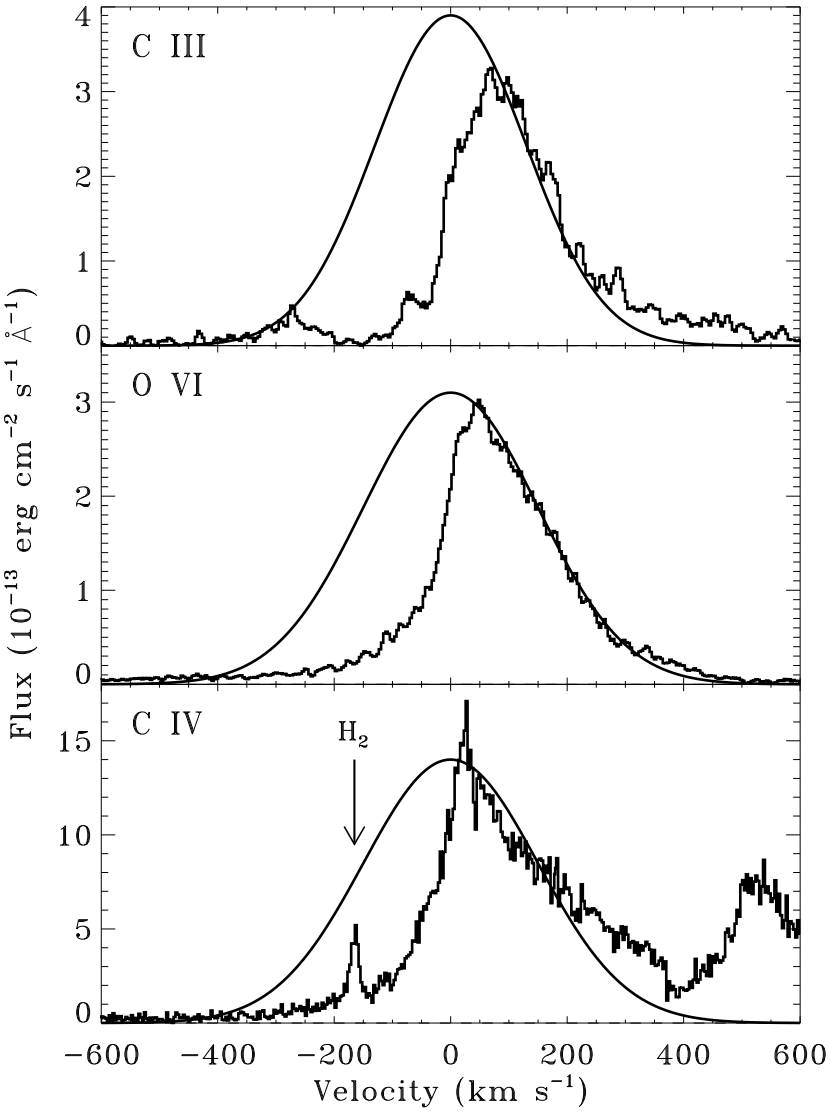

Fig. 2.— Line profiles of C III λ977, O VI λ1032, and C IV λ1548. Shown with each line is a Gaussian fit to the red side of the profile.

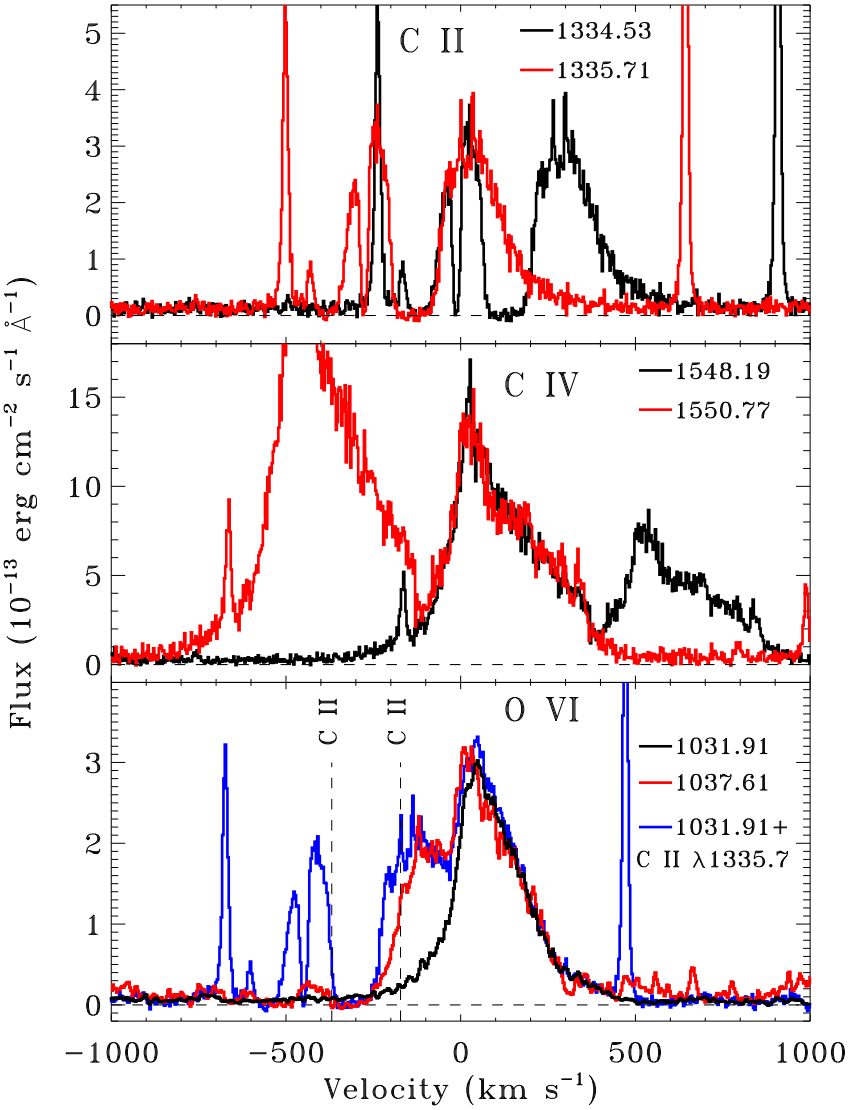

Fig. 3.— Line profiles of C II λ1335, C IV λ1550, and O VI λ1035. The black line shows the blue member of each multiplet. The red line shows the red member of each multiple scaled to match the peak and blue wing of the blue member. The dashed horizontal line marks the zero flux level. In the bottom panel, the blue line shows C II emission, scaled from the C II λ1335.7 line, added to the scaled O VI λ1032 line to estimate the profile of the C II λ1037 line.

Table 1: Continuum measurements near potential wind absorption features

Ion	λ (Å)	Continuum Regions[a] (Å)	Continuum Flux[b]
C III	977.0	973–975.5,979–985	3.8 ± 0.36
H I Lyβ	1025.7	1018–1023,1029.0–1030.7	4.93 ± 0.19
O VI	1031.9	1029.0–1030.7,1034.5–1035.5	5.05 ± 0.30
C II	1037.0	1034.5–1035.5,1042–1046.3	3.82 ± 0.17
O VI	1037.6	1034.5–1035.5,1042–1046.3	3.82 ± 0.17
C II	1335.0	1330–1333,1339-1342	13.2 ± 0.3
C IV	1549.0	1544.5–1546	23.8 ± 0.08

[a]Regions used to estimate the continuum flux at the respective emission line.
[b]10^{-15} ergs cm^{-2} s^{-1} Å^{-1}